

Ultralong-Range Rb-KRb Rydberg Molecules: Selected Aspects of Electronic Structure, Orientation and Alignment

Javier Aguilera-Fernández,¹ H. R. Sadeghpour,² Peter Schmelcher,^{3,4} and Rosario González-Férez¹

¹*Instituto Carlos I de Física Teórica y Computacional and Departamento de Física Atómica, Molecular y Nuclear, Universidad de Granada, 18071 Granada, Spain*

²*ITAMP, Harvard-Smithsonian Center for Astrophysics, Cambridge, Massachusetts 02138, USA*

³*The Hamburg Center for Ultrafast Imaging, Luruper Chaussee 149, 22761 Hamburg, Germany*

⁴*Zentrum für Optische Quantentechnologien, Universität Hamburg, Luruper Chaussee 149, 22761 Hamburg, Germany*

We investigate the structure and features of an ultralong-range triatomic Rydberg molecule formed by a Rb Rydberg atom and a KRb diatomic molecule. In our numerical description, we perform a realistic treatment of the internal rotational motion of the diatomic molecule, and take into account the Rb($n, l \geq 3$) Rydberg degenerate manifold and the energetically closest neighboring levels with principal quantum numbers $n' > n$ and orbital quantum number $l \leq 2$. We focus here on the adiabatic electronic potentials evolving from the Rb($n, l \geq 3$) and Rb($n = 26, l = 2$) manifolds. The directional properties of the KRb diatomic molecule within the Rb-KRb triatomic Rydberg molecule are also analyzed in detail.

I. INTRODUCTION

Recently the existence of a new class of ultralong-range polyatomic Rydberg molecules was predicted theoretically [1, 2]. These huge-sized Rydberg molecules are formed by a Rydberg atom and either a Λ -doublet or a rotating polar diatomic molecule [1, 3]. The binding mechanism is established by the electric field of the Rydberg electron and the ionic core that couples either the two internal states or hybridizes the rotational motion of the molecule due to its permanent electric dipole moment. The existence of these ultralong-range triatomic Rydberg molecules was predicted for polar diatomic molecules with subcritical electric dipole moments ($d_0 < 1.639$ D) in order to prevent the binding of the Rydberg electron to the heteronuclear (polar) diatomic molecule [4–7].

These giant Rydberg molecules possess an electronic structure characterized by oscillating Born-Oppenheimer potential curves evolving from the Rb($n, l \geq 3$) Rydberg manifold with binding energies of a few GHz. Their electronic structure could be controlled and manipulated by weak electric fields of a few V/cm [8]. The Rydberg-field-induced coupling gives rise to a strong hybridization of the angular motion of the diatomic molecule together with a strong orientation and alignment. In particular, the orientation of the diatomic molecule within the Rydberg molecule changes sign and strongly depends on the dominant contribution to the Rydberg electric field [1, 3]. The two internal rotational states of opposite orientation of the polar diatomic molecule could be coupled by means of a Raman scheme [1], which might allow for the switchable dipole-dipole interaction needed to implement molecular qubits [9].

Recently, we investigated electronic properties of the polyatomic Rydberg molecule composed of a Rb Rydberg atom and the KRb diatomic molecule [3]. Our theoretical description has included an explicit treatment of the angular degrees of freedom of the diatomic molecule within

the rigid-rotor approximation. Here, we extend this study on the Rb-KRb triatomic Rydberg molecule. We investigate the molecule and obtain Born-Oppenheimer potential (BOP) curves of the Rb($n, l \geq 3$)-KRb Rydberg molecule with varying principal quantum number n of the Rydberg electron and varying internuclear distance between the ionic core Rb⁺ and the diatomic KRb. The lowest-lying BOPs evolving from Rb($n, l \geq 3$) and KRb($N = 0$) present potential wells with depths of a few GHz. We also explore the adiabatic potentials of the Rydberg molecule formed by the KRb being in a rotational excited state, and the Rb($26d$) Rydberg manifold. These BOPs evolving from the Rb($26d$) state present wells with depths of a few MHz that support several vibrational bound states. This opens the possibility of creating these macroscopic Rydberg molecules by two-photon excitation of ground-state Rb in an ultracold mixture of Rb and KRb. The orientation and alignment of the diatomic molecule within the Rydberg molecule is also analyzed in terms of the contributions to the electric field due to the Rydberg electron and ionic core.

The paper is organized as follows. In section II we describe the adiabatic Hamiltonian of the triatomic Rydberg molecule. The electronic structure of a Rb-KRb Rydberg molecule is analyzed in detail in section III: We analyze the Born-Oppenheimer potentials evolving from the degenerate Rydberg manifolds Rb($n, l \geq 3$) and Rb($26d$), and the directional properties of the KRb diatomic molecule within the Rb-KRb Rydberg trimer. The conclusions are provided in section IV.

II. THE ADIABATIC MOLECULAR HAMILTONIAN

We consider a triatomic Rydberg molecule formed by a Rydberg atom and a diatomic heteronuclear molecule, which is located on the Z axis in the laboratory fixed frame (LFF) at a distance R from the ionic core, the

latter being placed at the origin of the LFF. The Born-Oppenheimer Hamiltonian reads

$$H_{ad} = H_A + H_{mol} \quad (1)$$

where H_A is the single electron Hamiltonian describing the Rydberg atom

$$H_A = -\frac{\hbar^2}{2m_e} \nabla_r^2 + V_l(r), \quad (2)$$

with $V_l(r)$ being the l -dependent model potential [11], and l the angular quantum number of the Rydberg electron.

The term H_{mol} is the Hamiltonian of the rotational motion of the diatomic molecule in the electric field due to the Rydberg electron and ionic core

$$H_{mol} = BN^2 - \mathbf{d} \cdot \mathbf{F}_{ryd}(\mathbf{R}, \mathbf{r}) \quad (3)$$

with \mathbf{N} being the molecular angular momentum operator, B the rotational constant, and \mathbf{d} the permanent electric dipole moment. Note that we describe the rotational motion of the diatomic molecule within the rigid-rotor approximation. The electric field created by the ionic core and Rydberg electron at position \mathbf{R} reads [1, 2]

$$F_{ryd}(\mathbf{R}, \mathbf{r}) = e \frac{\mathbf{R}}{R^3} + e \frac{\mathbf{r} - \mathbf{R}}{|\mathbf{r} - \mathbf{R}|^3} \quad (4)$$

with $\mathbf{R} = R\hat{Z}$. We consider all three spatial components of this electric field taking into account that the position of the polar molecule is fixed along the LFF Z -axis. For a detailed expression of this electric field, we refer the reader to Refs. [3, 10].

The orbital angular momentum of the Rydberg electron and the rotational angular momentum of the diatomic molecule are coupled to the total angular momentum of the Rydberg molecule (excluding an overall rotation) $\mathbf{J} = \mathbf{N} + \mathbf{l}$. For the considered configuration of the Rydberg molecule, the eigenstates are characterized by the magnetic quantum number M_J , which is the projection of \mathbf{J} onto the LFF Z -axis.

The Schrödinger equation associated with the Hamiltonian 1 is solved by a basis set expansion in the coupled basis

$$\begin{aligned} \psi_{nlN JM_J}(\mathbf{r}, \Omega_d) = & \sum_{m_l=-l}^{m_l=l} \sum_{M_N=-N}^{M_N=N} \langle l m_l N M_N | J M_J \rangle \\ & \times \psi_{nlm}(\mathbf{r}) \times Y_{NM_N}(\Omega_d) \end{aligned} \quad (5)$$

where $\psi_{nlm}(\mathbf{r})$ is the Rydberg electron wave function, $Y_{NM_N}(\Omega_d)$ the spherical harmonics representing the field-free rotational wave function of the diatomic molecule with the rotational and magnetic quantum numbers N and M_N , respectively, Ω_d the internal coordinates of the diatomic molecule, and $\langle l m_l N M_N | J M_J \rangle$ the Clebsch-Gordan coefficient. Taking into account the azimuthal

symmetry of the Rydberg molecule, the basis set expansion of the wave function reads

$$\Psi(\mathbf{r}, \Omega_d; R) = \sum_{n,l,N,J} C_{nlNJ}(R) \psi_{nlN JM_J}(\mathbf{r}, \Omega_d), \quad (6)$$

where we have explicitly indicated the dependence of the wave function and expansion coefficients $C_{nlNJ}(R)$ on the internuclear distance R between the diatomic molecule and the ionic core. For computational reasons, of course, we have to cut the infinite series (6) to a finite one. In this work, we have included the rotational excitations with $N \leq 6$ for KRb, and for Rb, the $(n, l \geq 3)$ degenerate manifold, and the energetically neighboring levels $(n+1)d$, $(n+2)p$, and $(n+3)s$. The quantum defect of the Rb(nf) Rydberg state has been neglected.

III. THE ELECTRONIC STRUCTURE OF THE RB-KRB RYDBERG MOLECULE

In this section, we investigate the electronic structure of the Rydberg molecule formed by a Rb atom and the heteronuclear molecule KRb with rotational constant $B = 1.114$ GHz [12], and electric dipole moment $d = 0.566$ D [13]. The interaction between the electric field created by the ionic core and Rydberg electron and the permanent electric dipole moment of KRb is responsible for the binding mechanism of Rb-KRb. The electric field (4) decreases as the distance between Rb^+ and KRb is increased, and, therefore, the coupling between the subsystems Rb and KRb also decreases. For large enough values of R , the adiabatic electronic potentials approach the energies of the uncoupled system $E_{nl} + BN(N+1)$, with E_{nl} being the energy of Rb(n, l), and $BN(N+1)$ the rotational energy of KRb in an eigenstate with rotational quantum number N .

A. The adiabatic potentials evolving from the Rb($n, l \geq 3$) degenerate manifold

The BOPs of the Rb-KRb molecule evolving from the Rydberg degenerate manifold Rb($n = 25, l \geq 3$) and with magnetic quantum numbers $M_J = 0$ and $M_J = 1$ are presented in Figure 1 (a) and Figure 1 (b), respectively. In this region of the spectrum, we encounter adiabatic states evolving from Rb(28s) and KRb in a rotationally excited state, which show a very weak dependence on the internuclear distance. This behavior is due to the small impact of the Rydberg electric field on the $N = 6$ excited state of KRb, which possesses a large field-free rotational energy. The electronic states evolving from the Rb($n = 25, l \geq 3$) manifold are shifted in energy from the uncoupled-system energy $E_{nl} + BN(N+1)$. These energy shifts strongly depend on the internuclear separation of Rb-KRb due to the interplay between the electric fields created by the Rydberg electron and the ionic core. They are of the range from a few to tens of

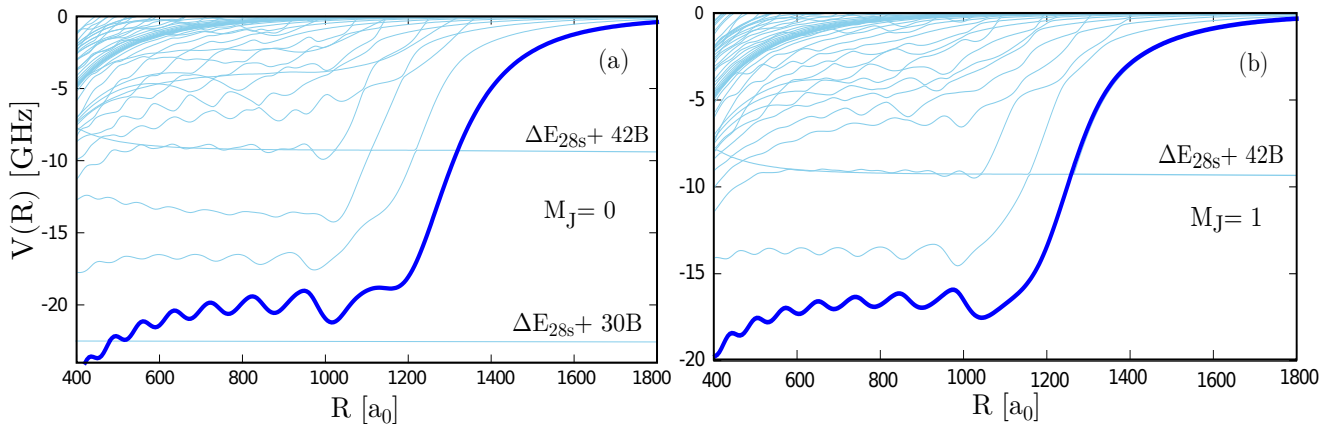


FIG. 1. For the Rb-KRb Rydberg molecule, the Born-Oppenheimer potentials as a function of the distance between KRb and Rb^+ for (a) $M_J = 0$ and (b) $M_J = 1$ are shown, specifically the BOP evolving from Rb($28s$) and KRb in a rotational excited state, and from the Rb($n = 25, l \geq 3$) manifold and the rotational ground state of Rb. The energetically lowest-lying adiabatic potentials evolving from the Rb($n = 25, l \geq 3$) manifold are shown with thicker lines. The zero energy has been set to the energy of the Rb($n = 25, l \geq 3$) degenerate manifold and the KRb ($N = 0$) state.

GHz. The BOPs oscillate as a function of R , and numerous avoided crossings among neighboring electronic states characterize the spectrum. For $R \sim 1000 a_0$, the energetically lowest-lying BOPs present potential wells of a few GHz depths, which support several vibrational states [3]. By further increasing R , the coupling between the Rydberg atom and KRb decreases, and the BOPs approach the asymptotic limit of the uncoupled system. Note that in these figures, the zero energy has been set at $E_{n=25, l \geq 3}$, i. e., for the uncoupled system KRb($N = 0$) and Rb($n = 25, l \geq 3$).

We focus now on the evolution of the electronic structure as the principal quantum number of the Rydberg degenerate manifold Rb($n, l \geq 3$) is increased. In Figure 2, we present the energetically lowest-lying adiabatic electronic states with $M_J = 0$ and $M_J = 1$ evolving from the Rb($n, l \geq 3$) manifolds for $n = 25, 26, 27, 29$, and 31 . These BOPs show a qualitatively similar oscillatory behavior as a function of R . By increasing the principal quantum number of the Rydberg manifold, some differences are observed. First, the energy shift of these BOPs from the degenerate manifold of the Rydberg atom decreases as n is increased. Second, the location of the potential wells is shifted towards larger values of the internuclear separation between Rb^+ and KRb. This is due to the radial extension of the electronic Rydberg wave function of Rb($n, l \geq 3$) which increases as n is enhanced. Third, the depth of the wells decreases with increasing n . The outermost potential well of the $M_J = 0$ BOPs is very shallow and do not support vibrational bound states. In contrast, the potential well with $M_J = 0$ located at the left of this outermost one is the deepest one supporting several bound states and with depths of several GHz for all the Rb($n, l \geq 3$)-KRb($N = 0$) molecules investigated here. For instance, we have found 7 and 6 vibrational bound states in these potential wells of these energetically lowest-lying Rb($n = 25, l \geq 3$) and Rb($n = 31, l \geq 3$)

BOPs with $M_J = 0$, respectively.

We analyze now the directional features of the KRb molecule within the Rb-KRb triatomic Rydberg molecule. For the lowest-lying electronic potentials evolving from the Rb($n = 25, l \geq 3$) and Rb($n = 29, l \geq 3$) manifolds and with $M_J = 0$, the orientation, $\langle \cos \theta_d \rangle$, and alignment, $\langle \cos^2 \theta_d \rangle$, of KRb along the LFF Z -axis are shown in Figure 3 (a) and Figure 3 (b), respectively. For the sake of simplicity, we only analyze the results for the Rb-KRb in these two manifolds, but qualitatively similar behavior is obtained for the others BOPs presented in Figure 2. We have computed the orientation and alignment of the rotational ground state of KRb in an electric field of varying field strength $5.14/R^2$ GV/cm, i. e., the strength of the electric field due to the Rydberg core, being parallel and antiparallel to the LFF Z -axis, see Figure 2. These results allow us to get a deeper physical insight into the interplay between the electric field due to the Rydberg electron and the Rb^+ core. For both BOPs, we encounter a regime where the electric field due to the Rydberg core is dominant, i. e., the total electric field is antiparallel to the LFF Z -axis, and KRb is anti-oriented. In this regime, the orientation of KRb within Rb-KRb is very close to the orientation of KRb in the $5.14/R^2$ GV/cm electric field. Let us comment, that for $R = 1000 a_0$, the electric field strength due to the Rydberg core is 5 kV/cm. The oscillations of the orientation of the KRb within Rb-KRb are due to the Rydberg electrons electric field, which oscillates resembling the behavior of its wave function. The amplitude of these oscillations increases as the Rydberg electrons electric field becomes more important. When the contribution of this field becomes dominant, the orientation of KRb changes sign and KRb becomes oriented along the Z -axis. The differences in the electronic Rydberg wave function of Rb($n = 29, l \geq 3$) and Rb($n = 25, l \geq 3$), are reflected in the fact that the KRb

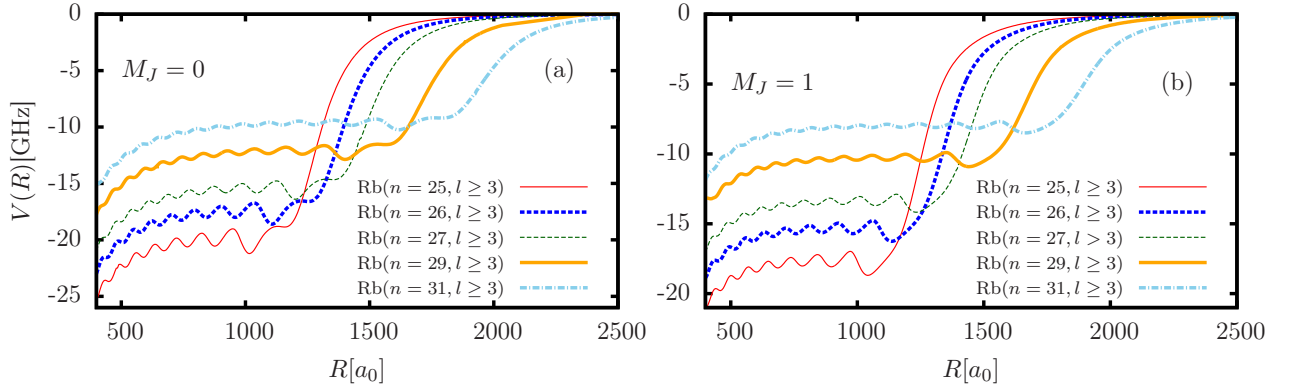


FIG. 2. For the Rb-KRb molecule, the energetically lowest-lying states with $M_J = 0$ and $M_J = 1$ evolving from the Rb($n, l \geq 3$) Rydberg manifold, for $n = 25, 26, 27, 29$, and 31 , and KRb in the rotational ground state $N = 0$ are shown. To facilitate the comparison, the zero energy has been set to the energy of the Rb($n, l \geq 3$) degenerate manifold and the KRb($N = 0$) level.

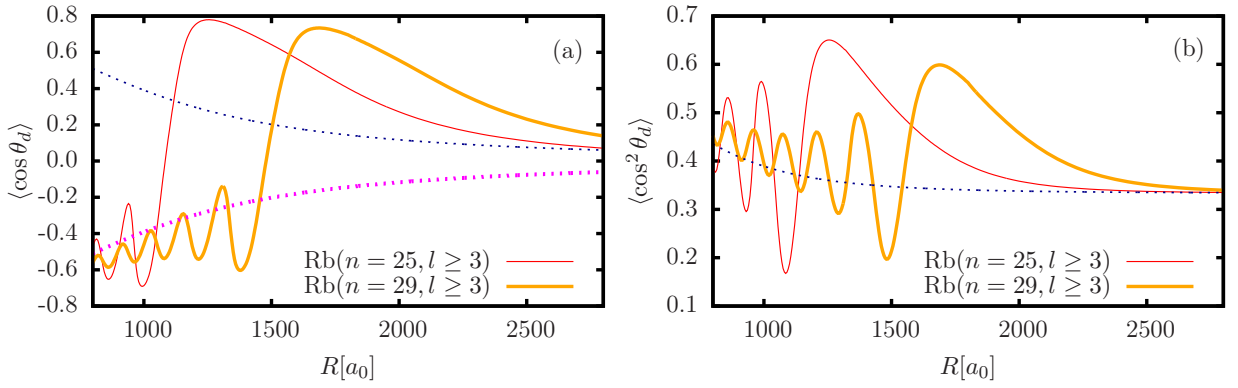


FIG. 3. For the KRb molecule within the energetically lowest-lying BOPs with $M_J = 0$ of Rb($n = 25, l \geq 3$)-KRb (thin solid) and Rb($n = 29, l \geq 3$)-KRb (thick solid), we show (a) the orientation $\langle \cos \theta_d \rangle$ and (b) the alignment $\langle \cos^2 \theta_d \rangle$ along the LFF Z -axis versus the internuclear distance between Rb $^+$ and KRb. We also present the orientation and alignment of KRb in an electric field parallel (thick dotted) and antiparallel (thin dotted) to the LFF Z -axis and strength $5.14/R^2$ GV/cm.

molecule is anti-oriented for a larger range of values of R for Rb($n = 29, l \geq 3$)-KRb($N = 0$). KRb is maximally oriented around the classical turning point $R \sim 2n^2 a_0$, and we have $\langle \cos \theta_d \rangle \approx 0.8$, which is the orientation of KRb in a strong electric field of 50 kV/cm strength [14]. The internuclear separation of Rb-KRb at which the KRb orientation reaches the maximum is shown versus the principal quantum number of the Rb($n, l \geq 3$) degenerate manifold in Figure 4. We observe a very good agreement with the $2n^2 a_0$ behavior. In Figure 4 we show also the internuclear separation of Rb-KRb at which the energetically lowest-lying BOP with $M_J = 0$ reaches the two outermost minima. The radial position of these two minima is shifted to lower values of R compared to the maximum of the KRb orientation. By further increasing R , the orientation decreases towards zero and approaches the orientation of KRb in the $5.14/R^2$ GV/cm electric field. Note that in the absence of an electric field, the KRb molecule is not oriented.

The alignment along the LFF Z -axis of KRb within Rb-KRb also shows an oscillatory behavior around the alignment of the KRb in a $5.14/R^2$ GV/cm electric field,

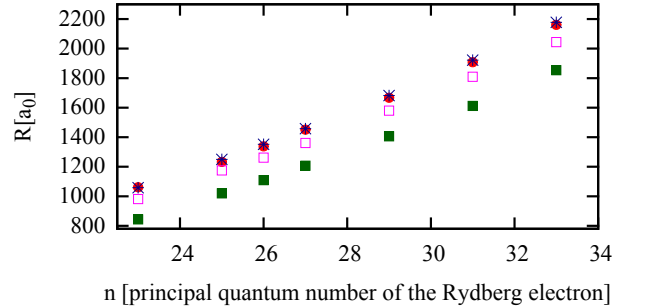


FIG. 4. For the Rb-KRb Rydberg molecule, we show the distance between the Rb $^+$ core and KRb (\bullet) at which the orientation of KRb is maximal within the lowest-lying $M_J = 0$ adiabatic potentials evolving from the Rb($n, l \geq 3$) manifolds for varying principal quantum number n . For these lowest-lying BOPs, we also present the internuclear separation R of Rb-KRb at which the one before the outermost (\square) and the outermost (\blacksquare) potential wells reach the minimum value. For comparison, we show the classical turning point $R \sim 2n^2 a_0$ (\star).

cf. Figure 3 (b). As the coupling of the dipole moment of KRb with the electric field due to the Rydberg electron becomes dominant compared to the coupling with the Rb^+ electric field, the amplitude of the oscillations become very large. When the distance of KRb from the Rb^+ core is large, the alignment approaches the field-free value $\langle \cos^2 \theta_d \rangle \approx 0.3333$.

B. The adiabatic potentials evolving from the $\text{Rb}(26d)$ Rydberg state

In the absence of an external electric field, the ultralong-range Rydberg molecule could be created from an ultracold mixture of Rb and KRb, by exciting the Rb from the ground-state to a nd Rydberg level in a two-photon process. In this section, we investigate the BOPs of the Rydberg molecule formed from $\text{Rb}(26d)$.

The adiabatic potentials with $M_J = 0$ evolving from the $\text{Rb}(26d)$ Rydberg states and the diatomic molecule in the rotational excitations $N = 2, 3$ and 4 are present in Figure 5. There are 5 electronic states with $M_J = 0$ and total angular momentum $J = 2 - N, \dots, N + 2$ in the uncoupled system. These BOPs show either a strong or a weak dependence on R , and when R is increased beyond a certain value they approach the energetical limit $\Delta E_{26d} + BN(N + 1)$, with $N = 2, 3$ and 4 and $\Delta E_{26d} = |E_{24,3} - E_{26d}|$. The BOPs with oscillatory behavior possess potential wells having depths of a few MHz or tens of MHz. These potential wells are deep enough to accommodate at least one vibrational level in which the polyatomic Rydberg molecule would exist. For a few vibrational levels, the square roots of the wave functions are shown in the potential wells in Figure 5. For the BOPs evolving from the $N = 3$ and $N = 4$ rotational states of KRb, we encounter several vibrational bound states with wave functions extending over several potential wells.

In Figure 5 (d), we present the orientation of the diatomic molecule along the LFF Z -axis for the electronic potentials evolving from the $\text{Rb}(26d)$ Rydberg manifold and KRb ($N = 3$). The diatomic molecule is weakly oriented along the LFF Z -axis, and similar results are obtained for the BOPs evolving from the diatomic molecule in the rotational excitations $N = 2$ and $N = 4$. This weak orientation can be explained in terms of the small impact of the Rydberg electric field on the rotational excited state, which is smaller than for the rotational ground state due to its larger rotational energy [14]. Thus, the weaker the coupling between the N rotational state and the neighboring levels $N \pm 1$, the smaller the orientation is.

IV. CONCLUSIONS

In this work, we have considered the ultralong-range Rydberg molecule formed by the KRb diatomic molecule

and the Rydberg Rb atom. The coupling mechanism of this triatomic Rydberg molecule is based on the interaction between the electric field produced by the Rydberg electron and core and the permanent electric dipole moment of the polar molecule. We have performed an analysis of the electronic structure of Rb-KRb when the Rb atom is in the Rydberg degenerate manifold ($n, l \geq 3$), with $n = 25, 26, 27, 29$, and 31. These adiabatic potentials show an oscillatory behavior as a function of the separation between Rb^+ and KRb. For the $\text{Rb}(n, l \geq 3)$ -KRb($N = 0$) molecules, the lowest-lying BOPs show potential wells of a few GHz depths. As the principal quantum number of the Rydberg excitation n is enhanced, the depths of these potential wells decrease and their positions are shifted towards larger values of the internuclear separation R . These features reflect the oscillatory structure of the Rydberg electronic wave function.

We have also investigated the properties of the Rydberg molecule formed by the $\text{Rb}(26d)$ Rydberg state and the diatomic molecule in an excited rotational state. BOPs with both an oscillatory and a smooth behavior as function of R are encountered. For $\text{Rb}(26d)$ -KRb(N), these oscillatory BOPs present potential wells with depths of a few tens of MHz, which can accommodate a number of bound vibrational states. These results demonstrate that these ultralong-range Rydberg molecules could be created by a standard two-photon excitation of ground state Rb in an ultracold mixture of Rb and KRb.

Due to the electric field of the Rydberg electron and core, the directional properties of the KRb molecule within the Rb-KRb triatomic molecule are significantly affected. The orientation and alignment of KRb has been analyzed in terms of the contribution of the electric fields due to the Rydberg electron and ionic core. Within these BOPs, the polar diatomic molecule presents two opposite orientations along the LFF Z -axis with its electric dipole moment pointing either toward or away from the ionic core.

ACKNOWLEDGMENTS

RGF and JAF gratefully acknowledge financial support by the Spanish projects FIS2014-54497-P (MINECO), P11-FQM-7276 (Junta de Andalucía), and by the Andalusian research group FQM-207. We also acknowledge financial support by the Initial Training Network COHERENCE of the European Union FP7 framework. HRS and PS acknowledge ITAMP at the Harvard-Smithsonian Center for Astrophysics for support.

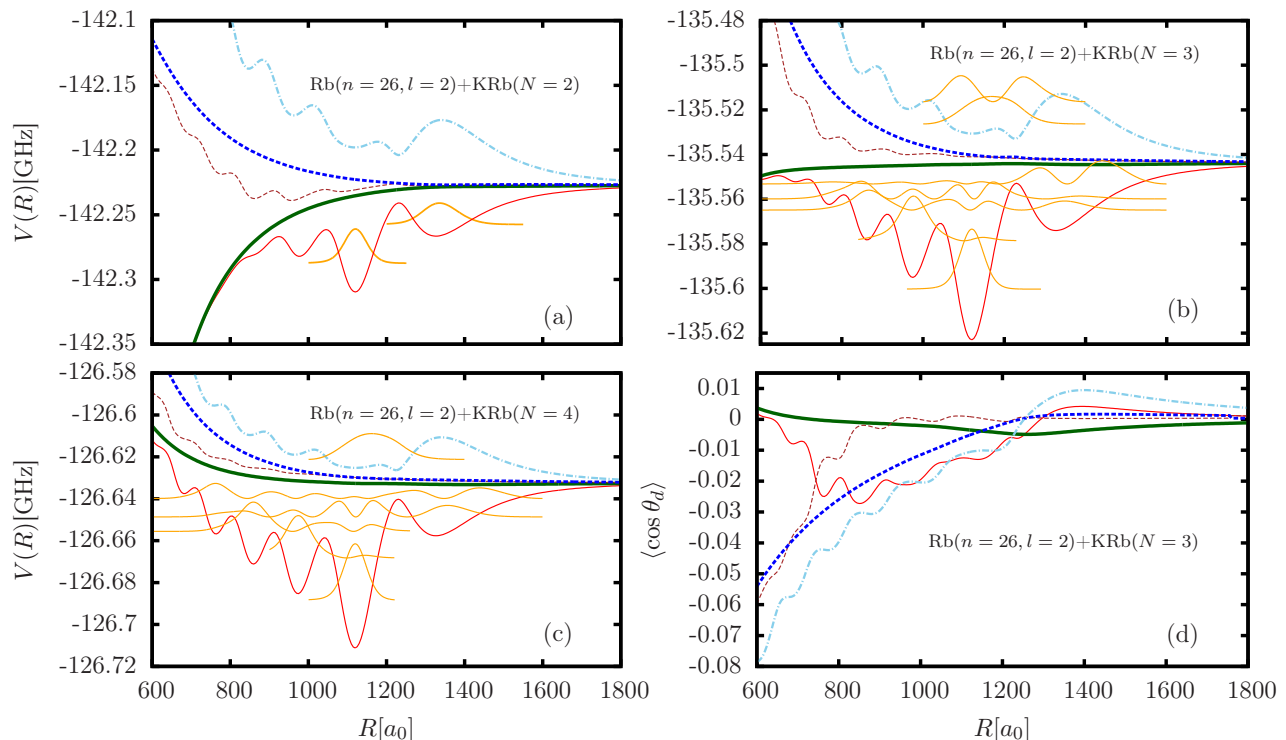


FIG. 5. For the Rb-KRb Rydberg molecule, Born-Oppenheimer potentials with $M_J = 0$ evolving from the Rb($26d$) state and KRb in the rotational levels (a) $N = 2$, (b) $N = 3$, and (c) $N = 4$. We have plotted the 5 electronic states with $M_J = 0$ and total angular momentum $J = 2 - N, \dots, N + 2$ in the uncoupled system. In the potentials wells, the square of the vibrational wave functions are shown in arbitrary units. The zero energy has been set to the energy of the Rb($n = 25, l \geq 3$) degenerate manifold and the KRb ($N = 0$) state. In panel (d), we show the orientation along the LFF Z -axis of KRb within the BOPs of the Rydberg molecule Rb($26d$)-KRb($N = 3$).

-
- [1] S.T. Rittenhouse and H.R. Sadeghpour, Phys. Rev. Lett. **104**, 243002 (2010)
- [2] S.T. Rittenhouse, M. Mayle, P. Schmelcher and H.R. Sadeghpour, J. Phys. B **44**, 184005 (2011)
- [3] R González-Férez, H.R. Sadeghpour, and P. Schmelcher, New J. Phys. **17**, 013021 (2015)
- [4] E. Fermi and E. Teller, Phys. Rev. **72**, 399 (1947)
- [5] J.E. Turner, Am. J. Phys. **45**, 758 (1977)
- [6] C.W. Clark, Phys. Rev. A **20**, 1875 (1979)
- [7] H. Hotop, M.-W. Rul, and I.I. Fabrikant, Physica Scripta **2004**, 22 (2004)
- [8] M. Mayle, S.T. Rittenhouse, P. Schmelcher and H.R. Sadeghpour, Phys. Rev. A **85**, 052511 (2012)
- [9] E. Kuznetsova, R. Côté, K. Kirby, and S. F. Yelin, Phys. Rev. A **78**, 012313 (2008)
- [10] K. Ayuel and P. de Chatel, Physica B **404**, 1209 (2009)
- [11] M. Marinescu, H. R. Sadeghpour, and A. Dalgarno, Phys. Rev. A **49**, 982 (1994)
- [12] K.-K. Ni, S. Ospelkaus, D.J. Nesbitt, J. Ye, and D.S. Jin, Phys. Chem. Chem. Phys. **11**, 9626 (2009)
- [13] K.-K. Ni, S. Ospelkaus, M.H.G. de Miranda, A. Pe'er, B. Neyenhuis, J.J. Zirbel, S. Kotochigova, P.S. Julienne, D.S. Jin and J. Ye, Science **322**, 231 (2008)
- [14] R. González-Férez, M. Mayle, P. Sánchez-Moreno, and P. Schmelcher, Eur. Phys. Lett. **83**, 43001 (2008)